Co-operation between different targeting pathways during integration of a membrane protein

Keller, Rebecca; de Keyzer, Jeanine; Driessen, Arnold J. M.; Palmer, Tracy

Published in:
Journal of Cell Biology

DOI:
10.1083/jcb.201204149

Publication date:
2012

Published October 8, 2012

Co-operation between different targeting pathways during integration of a membrane protein

Rebecca Keller,[1] Jeanine de Keyzer,[2] Arnold J.M. Driessen,[2] and Tracy Palmer[1]

[1]Division of Molecular Microbiology, College of Life Sciences, University of Dundee, Dundee DD1 5EH, Scotland, UK
[2]Divison of Molecular Microbiology Groningen Biomolecular Sciences and Biotechnology Institute and Zernike Institute for Advanced Materials, University of Groningen, 9747 AG Groningen, Netherlands

Membrane protein assembly is a fundamental process in all cells. The membrane-bound Rieske iron-sulfur protein is an essential component of the cytochrome bc_1 and cytochrome b_6f complexes, and it is exported across the energy-coupling membranes of bacteria and plants in a folded conformation by the twin arginine protein transport pathway (Tat) transport pathway. Although the Rieske protein in most organisms is a monotopic membrane protein, in actinobacteria, it is a polytopic protein with three transmembrane domains. In this work, we show that the Rieske protein of *Streptomyces coelicolor* requires both the Sec and the Tat pathways for its assembly. Genetic and biochemical approaches revealed that the initial two transmembrane domains were integrated into the membrane in a Sec-dependent manner, whereas integration of the third transmembrane domain, and thus the correct orientation of the iron-sulfur domain, required the activity of the Tat translocase. This work reveals an unprecedented co-operation between the mechanistically distinct Sec and Tat systems in the assembly of a single integral membrane protein.

Introduction

Protein transport into and across biological membranes is an essential function for all cells. In bacteria this is achieved by distinct transport machineries that operate in parallel. These machineries are also present in the cytoplasmic membranes of archaea and the thylakoid membranes of plant chloroplasts. The Sec (general secretory) pathway transports unfolded proteins (for review see Driessen and Nouwen, 2008). The Sec translocon comprises a heterotrimeric complex of SecYEG, which forms a narrow channel of sufficient diameter to accommodate unfolded polypeptide chains. Proteins are targeted to the Sec translocon by two different routes. The SecB chaperone acts posttranslationally to target soluble substrate proteins to the Sec translocon, where translocation is driven by the ATPase SecA. In contrast, the signal recognition particle (SRP) interacts with hydrophobic Sec substrates, binding to hydrophobic α-helical stretches as they emerge from the ribosome. SRP guides substrates to the Sec translocon in a cotranslational manner, and substrates are threaded into the Sec channel from the translating ribosome. The vast majority of bacterial inner membrane proteins are assembled cotranslationally, with the hydrophobic α-helices proposed to escape into the lipid bilayer through a lateral gate in the Sec translocon (Van den Berg et al., 2004). Some Sec-dependent inner membrane proteins require an additional protein, YidC, for their correct assembly. YidC interacts with the transmembrane segments of newly synthesized membrane proteins as they exit the SecYEG complex (Scotti et al., 2000), and is presumed to assist in insertion (du Plessis et al., 2006) and in correct folding (Nagamori et al., 2004). In addition, however, YidC can also function as an independent membrane protein insertase and assists in membrane protein integration of relatively small, usually monotopic membrane proteins (van der Laan et al., 2004a; Serek et al., 2004).

The twin-arginine protein transport (Tat) pathway is the second general protein export machinery that resides in the bacterial cytoplasmic membrane. The Tat machinery, in contrast to Sec, transports folded substrate proteins. Tat substrates, like almost all exported Sec substrates, are synthesized with N-terminal signal peptides that are usually cleaved during the export process by an externally facing signal peptidase

Correspondence to Rebecca Keller: r.keller@dundee.ac.uk; or Tracy Palmer: t.palmer@dundee.ac.uk

Abbreviations used in this paper: IMV, inner membrane vesicle; MBP, maltose-binding protein; Sec, general secretory pathway; SRP, signal recognition particle; Tat, twin arginine protein transport pathway; TM, transmembrane domain.

Supplemental Material can be found at:
http://jcb.rupress.org/content/suppl/2012/10/04/jcb.201204149.DC1.html

The Rockefeller University Press $30.00
J. Cell Biol. Vol. 199 No. 2 303–315
www.jcb.org/cgi/doi/10.1083/jcb.201204149

Published October 8, 2012

(Cline and Theg, 2007; for review see Palmer and Berks, 2012). Although superficially similar, there are several differences between Sec and Tat signal peptides, including the presence of a conserved S-R-R-x-F-L-K twin arginine motif in Tat signals where the arginines are almost always invariant, and are essential for efficient transport by the Tat pathway (Berks, 1996; Stanley et al., 2000). The Tat pathway can also assemble a few membrane proteins. In *Escherichia coli* there are five Tat-dependent membrane proteins, each of which has a single transmembrane helix at its C terminus. The thylakoid Tat pathway can also integrate membrane proteins (Summer et al., 2000; Molik et al., 2001). There appears to be no requirement for YidC for the correct integration of *E. coli* membrane-bound Tat substrates (Hatzixanthis et al., 2003).

A major subset of Tat substrate proteins is those that contain redox cofactors, such as iron-sulfur clusters or the molybdenum cofactor. Complex biosynthetic pathways exist in the cytoplasm to assemble such substrates, and their folded state precludes transport by the Sec pathway (for review see Sargent, 2007). One of the most important Tat substrates in bacteria and plants is the Rieske iron-sulfur protein. The Rieske protein is an essential component of the cytochrome bc_1 and b_6f complexes of many photosynthetic and respiratory electron transport chains, and plays a fundamental role in bacterial and plant physiology. In most organisms the Rieske protein has an N-terminal signal anchor that is recognized by the Tat machinery, which is linked via a flexible hinge region to the conserved iron-sulfur cluster–containing globular domain. In bacteria and plant thylakoids, the assembly of the Rieske protein into the membrane is strictly Tat dependent (Molik et al., 2001; Bachmann et al., 2006; De Buck et al., 2007).

Interestingly, the Rieske proteins of Gram-positive actinobacteria appear to be substantially larger and more hydrophobic than those of other bacteria (Niebisch and Bott, 2001, 2003). Sequence alignment of the Rieske proteins from representative examples of the class including *Corynebacterium glutamicum*, *Streptomyces coelicolor*, and *Mycobacterium tuberculosis* show that the proteins have three predicted transmembrane regions preceding the conserved iron-sulfur domain (Fig. 1). A canonical twin arginine motif is positioned adjacent to transmembrane domain 3, and a less conserved sequence containing a lysine-arginine pair is found adjacent to a transmembrane helix one. In this study we investigated which protein transport systems are involved in the correct assembly of the *S. coelicolor* Rieske protein. Our results indicate that the Sec and Tat pathways along with YidC participate to insert the three hydrophobic domains into the membrane.

Results

The Tat machinery recognizes an internal twin arginine motif in Sco2149 adjacent to the third transmembrane domain

The Tat pathway is found in most prokaryotes and in the thylakoid membranes of plants, and where examined it has been shown to be required for assembly of the Rieske protein into the membrane (Molik et al., 2001; Bachmann et al., 2006; De Buck et al., 2007). It should be noted however that the mitochondria of yeast and almost all nonphotosynthetic eukaryotes for which genome sequences are available lack the Tat pathway and require an AAA-ATPase, Bcs1, for Rieske protein translocation (Wagener et al., 2011). Previous proteomic analysis has shown that the *S. coelicolor* Rieske protein, Sco2149, was present in cell wall washes of the *S. coelicolor* wild-type strain but not of the *tatC* mutant strain (Widdick et al., 2006), which is consistent with this protein being a Tat substrate. However, it is not known whether the Tat pathway was required to assemble all three transmembrane domains of Sco2149 into the membrane or whether it recognized only part of the protein.

We therefore sought to investigate features of the *S. coelicolor* Rieske protein required for recognition by the Tat pathway. To this end, we constructed two fusion proteins that could be used as reporters for the Tat pathway in the heterologous organism *E. coli*. First, we replaced the globular iron-sulfur domain of Sco2149 with the mature domain of *E. coli* maltose-binding protein (MBP) to give construct TM123-MBP (Fig. 2 A). Previous work has shown that MBP, which is normally a Sec substrate, can be rerouted to the Tat pathway if fused to a Tat signal peptide (Blaudeck et al., 2003). As shown in Fig. 2 B, induction of expression of this fusion construct resulted in the ability of an *E. coli* strain lacking a chromosomally encoded copy of MBP to ferment maltose, as indicated by acidification of the growth medium detected with the pH indicator dye bromocresol purple. This indicates that the MBP portion of the fusion protein must reside at the periplasmic side of the membrane. If the same strain is rendered tat^- by introduction of a *tatABC* deletion allele, the strain can no longer ferment maltose, and the pH indicator dye remains purple, demonstrating that the translocation of MBP is dependent on the Tat pathway.

As a second reporter, we removed the MBP reporter and replaced it with the mature region of the *E. coli* Tat substrate, AmiA, to give TM123-AmiA (Fig. 2 A). AmiA, along with a related protein AmiC, are two Tat-dependent amidases that are responsible for cell wall remodeling during growth. *E. coli* strains where the Tat system is inactive or tat^+ strains lacking AmiA and AmiC fail to grow in media containing SDS because of a leaky cell envelope (Ize et al., 2003). Introduction of the TM123-AmiA fusion protein into an *E. coli* strain lacking periplasmic AmiA and AmiC allowed the strain to grow on media supplemented with SDS, indicating that the AmiA protein is localized to the periplasmic side of the membrane (Fig. 2 C). It should be noted that growth supported by this construct was rather poor, probably because the AmiA domain is anchored to the cytoplasmic membrane rather than being free in the periplasm, where it can presumably more easily access the peptidoglycan. Indeed, the ability of this fusion protein to support growth on SDS was enhanced if the signal peptidase I cleavage site of AmiA was also included in the construct, which should allow release of the amidase from the membrane. In both cases, export of the amidase domain of the fusion protein was fully Tat dependent, as no growth was observed if the strain was additionally deleted for *tatABC* (Fig. 2 C).

Alignment of amino acid sequences of actinobacterial Rieske proteins (Fig. 1) shows that there is a highly conserved

Published October 8, 2012

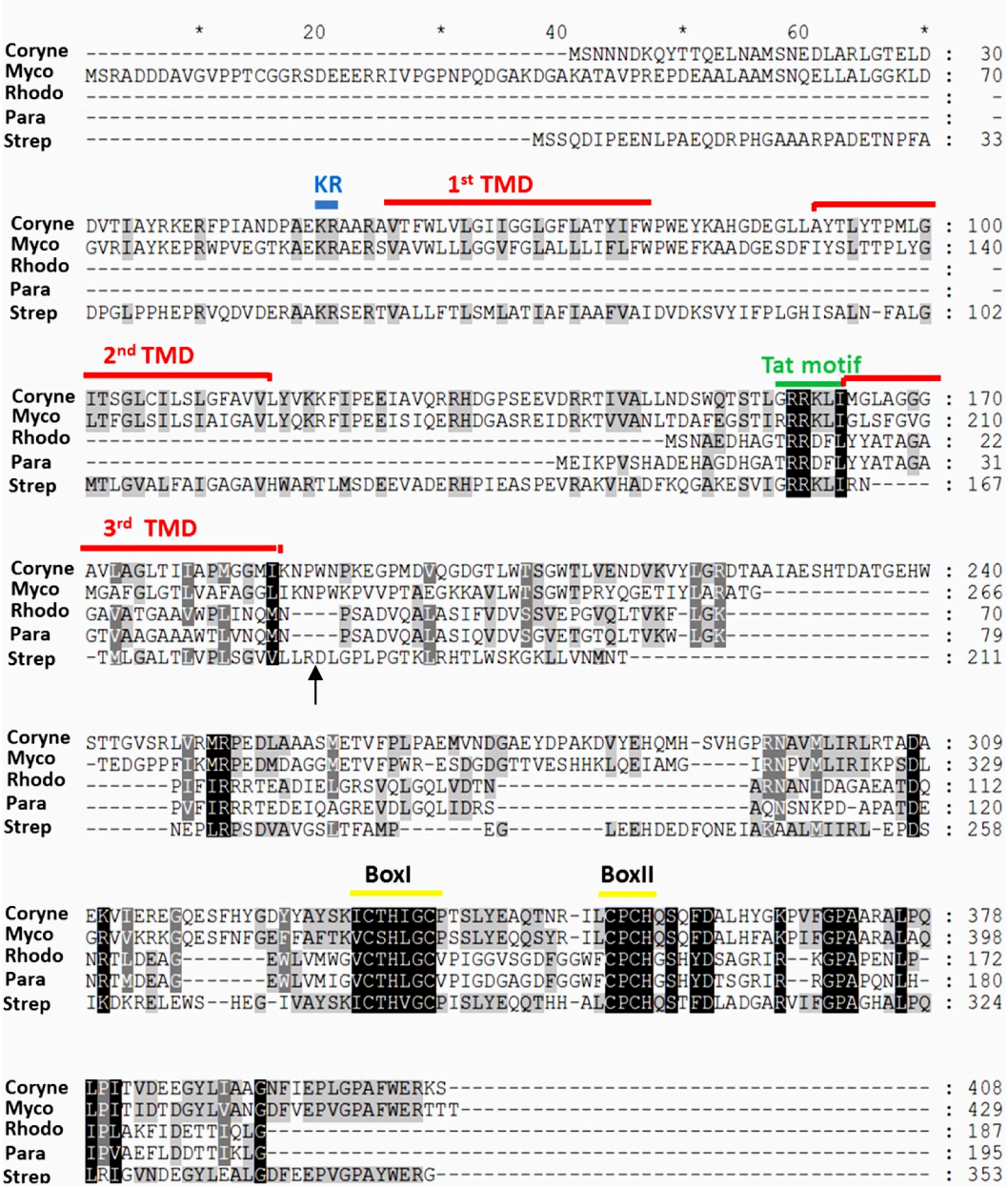

Figure 1. **The actinobacterial Rieske proteins.** Protein sequence alignments of the Rieske iron-sulfur proteins from different bacteria. Proteins were aligned using ClustalW and GENEDOC. The longer Rieske iron-sulfur proteins of actinobacterial representatives *C. glutamicum* (Coryne), *M. tuberculosis* (Myco), and *S. coelicolor* (Strep) are aligned alongside the well-characterized Rieske proteins of *Paracoccus denitrificans* (Para) and *Rhodobacter sphaeroides* (Rhodo). Transmembrane domains (TMD) were predicted using TM2HMM (http://www.cbs.dtu.dk/services/TMHMM/) and are marked in red above the alignment. The consensus twin arginine (Tat) motif is highlighted in green and a KR motif in front of the first predicted TMD is indicated in blue. Conserved boxes I and II that coordinate the 2Fe-2S cluster are highlighted in yellow. The arrow indicates the position after which the reporter proteins MBP or AmiA were fused. The differences in shading (from gray to black) refer to the level of amino acid conservation between the different species (with black indicating absolute conversion).

twin arginine motif directly preceding the third predicted transmembrane domain (TM3) that closely resembles the Tat-targeting consensus sequence. In addition there is a lysine-arginine motif that is found adjacent to the first transmembrane domain (TM1). This is less well conserved; for example, it is a lysine-histidine pair in *Streptomyces griseoaurantiacus,* an alanine-arginine pair in *Kytococcus sedentarius* DSM 20547, and a lysine threonine pair in *Clavibacter michiganensis* subspecies *michiganensis*. It has been shown that certain amino acids other than arginines can sometimes be tolerated within the twin arginine signal sequence, and indeed the Rieske proteins from plant thylakoids have a lysine-arginine pairing rather than the consecutive arginines that are generally found for the bacterial Rieske proteins. Therefore, to test which of these sequences was important for recognition of the protein by the Tat pathway, we constructed substitutions of either of the twin arginine residues before TM3 or the lysine-arginine pairing before TM1 to twin lysines ($TM12_{KK}$3-MBP or $_{KK}$TM123-MBP, respectively), using standard molecular biology

Published October 8, 2012

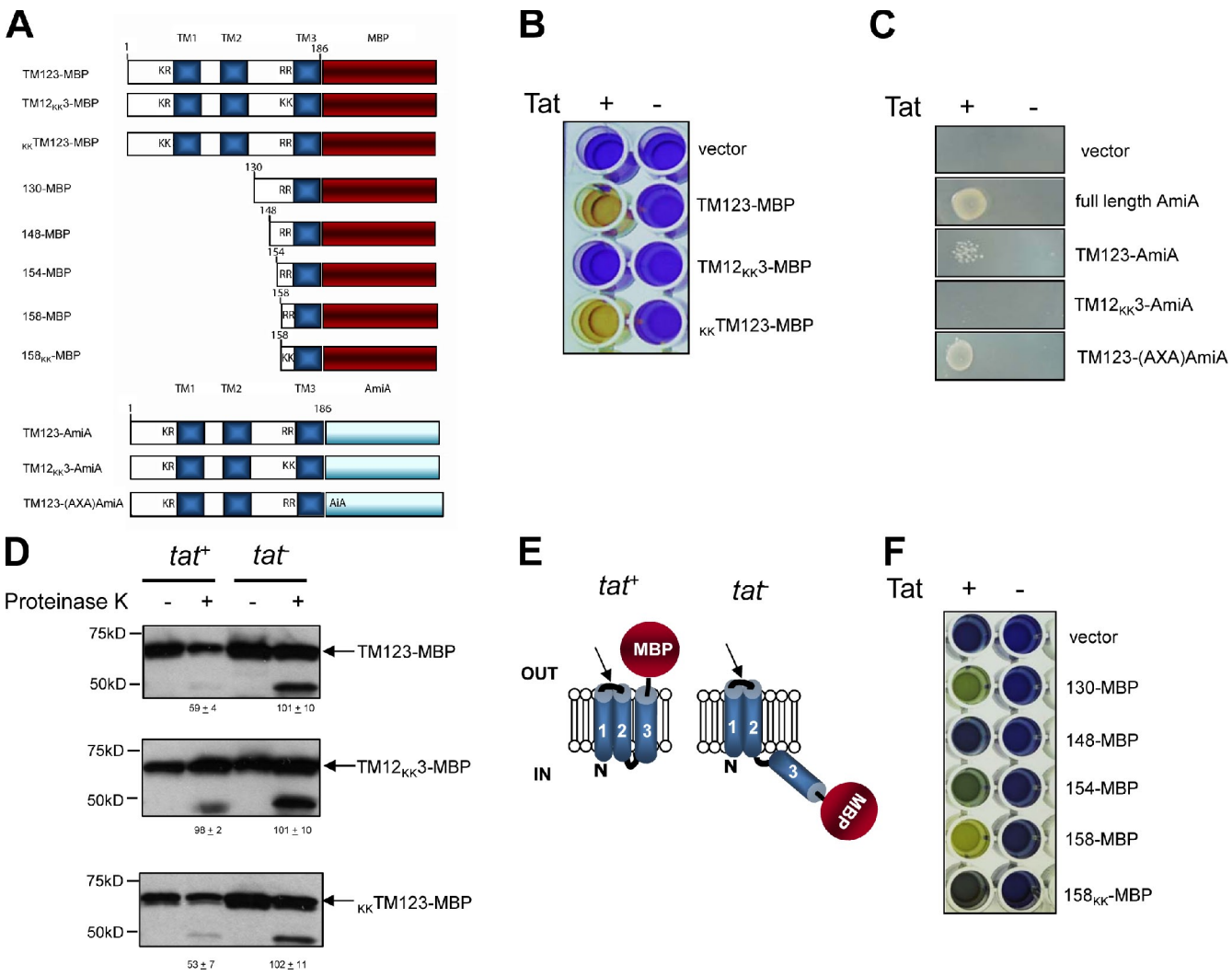

Figure 2. **Tat-dependent translocation of reporter proteins fused to the transmembrane domains of the *S. coelicolor* Rieske protein.** (A) Schematic representation of the constructs used in these experiments. Amino acid numbers are indicated. (B) Tat-dependent translocation of MBP fused to the hydrophobic portion of Sco2149. *E. coli* strain HS3018-A (deleted for *malE*) and an otherwise isogenic *tatABC* mutant strain containing either pBAD24 (vector), pBAD24 producing the Sco2149-MBP fusion protein (TM123-MBP), or variants of this construct where the twin arginine motif before TM3 or the lysine-arginine motif before TM1 were substituted to twin lysines ($TM12_{KK}3$-MBP or $_{KK}$TM123-MBP, respectively) were cultured on maltose indicator broth containing bromocresol purple, as described in Materials and methods. (C) Tat-dependent translocation of AmiA fused to the hydrophobic portion of Sco2149. *E. coli* strain MCDSSAC (which carries chromosomal deletions in the signal peptide coding regions of *amiA* and *amiC*) and its cognate *tatABC* mutant containing either pSU18 (vector), pSU18 producing native AmiA (AmiA), pSU18 producing the Sco2149-AmiA fusion protein (TM123-AmiA), or variants of this construct where the twin arginine motif before TM3 was substituted to twin lysines or where the native AmiA signal peptidase cleavage site was present ($TM12_{KK}3$-AmiA or TM123-(AXA)AmiA, respectively) were cultured on LB medium containing 1% SDS as described in Materials and methods. (D) Proteinase K accessibility of the TM123-MBP fusion protein in right-side-out membrane vesicles. Sphaeroplasts were prepared from HS3018-A or HS3018-AΔ*tatABC* strains producing TM123-MBP, $TM12_{KK}3$-MBP, or $_{KK}$TM123-MBP. Samples were treated with proteinase K, precipitated with TCA, and analyzed via immunoblotting using anti-MBP antiserum. The numbers beneath the lanes are the percentage of full-length fusion protein remaining after proteinase K treatment (±SD, where $n = 6$ for the TM123-MBP samples and $n = 3$ for the $TM12_{KK}3$-MBP and $_{KK}$TM123-MBP samples). (E) Proposed topologies of TM123-MBP in *tat*$^+$ and *tat*$^-$ strains of *E. coli*. The arrow indicates a probable protease accessible site in the periplasmic loop region between TM1 and TM2. (F) TM3 of Sco2149 alone can act as a Tat-targeting sequence. *E. coli* strain HS3018-A and an isogenic *tatABC* mutant containing either pBAD24 (vector) or pBAD24 producing variants of a Sco2149-MBP fusion protein containing an initiating methionine, and then the amino acids of Sco2149 (130–186 [130-MBP], 148–186 [148-MBP], 154–186 [154-MBP], and 158–186 [158-MBP]) fused to the mature region of MBP were cultured on maltose indicator broth containing bromocresol purple as described in Materials and methods. As an additional control, the twin arginine motif of construct 158-MBP was mutated to twin lysine (158_{KK}-MBP) and also tested for the ability to support metabolism of maltose.

techniques. It should be noted that replacement of the twin arginines for two consecutive lysine residues fully abolishes Tat-dependent transport of almost all reporter proteins tested. We then assessed the effects of these mutations on the localization of the reporter domains of the Sco2149 fusion proteins.

As shown in Fig. 2 (B and C), substitution of the twin arginines that are located close to TM3 for twin lysines abolished the translocation of either MBP or AmiA to the periplasmic side of the membrane because the cells could no longer grow fermentatively with maltose or survive in the presence of SDS. This strongly suggests that the conserved twin arginine motif is indeed recognized by the Tat machinery. In contrast, substitution of the lysine-arginine motif close to TM1 was without effect on the ability of the TM123-MBP fusion protein to support

Published October 8, 2012

maltose fermentation, which suggests that this motif is not required for Tat-dependent translocation of the globular domain.

To support the results of these growth tests, we isolated spheroplasts and assessed the accessibility of the MBP domain to proteinase K digestion by Western blotting using anti-MBP antiserum. As shown in Fig. 2 D, in the wild-type strain a proportion (~40%) of the TM123-MBP construct was sensitive to proteinase K digestion, confirming that the MBP domain resides at the periplasmic side of the membrane. A similar observation was also seen for the construct with a twin lysine pair replacing the lysine-arginine motif before TM1 ($_{KK}$TM123-MBP), which confirms that this is assembled in a similar way to the nonsubstituted construct. Because the control periplasmic protein leader peptidase was fully protease sensitive in these experiments (Fig. S1), we ascribe the incomplete digestion of the TM123-MBP construct to inefficient translocation of the protein. Alternatively it may reflect the fact that mature MBP is highly resistant to protease (Weiss et al., 1989). When either TM123-MBP or $_{KK}$TM123-MBP was produced in a *tat* mutant strain, a substantial proportion of the protein was no longer digested by proteinase K. Interestingly, however, a fraction of the protein was digested to produce a degradation product of ~49 kD that must contain at least some of the MBP domain because it cross-reacts with the antiserum. We ascribe this to cleavage at a weakly accessible protease site that lies in the P1 loop between TMs 1 and 2, and protection of the MBP domain is observed presumably because it is located at the cytoplasmic side of the membrane (Fig. 2 D). If this is the case, it would suggest that the first two transmembrane domains of Sco2149 are integrated into the membrane in a Tat-independent manner.

A rather different pattern of protease accessibility was observed when spheroplasts producing the TM123-MBP construct harboring the twin lysine substitution of the twin arginines preceding TM3 were examined. In this case, even when the Tat system was present, much of the construct was not digested by the protease. However, a fraction of the protein was digested to give a similar ~49-kD cross-reacting band to that seen for the unsubstituted construct when the Tat machinery was absent (Fig. 2 D). This observation therefore fully supports our previous conclusions that the Tat machinery recognizes the twin arginine motif before TM3.

Collectively, the results presented in Fig. 2 (B–D) indicate that the Tat machinery specifically recognizes a targeting sequence that lies at the N-terminal end of TM3. To confirm this, we designed a series of constructs expressing only the third transmembrane domain of Sco2149 fused to MBP and tested them for Tat-dependent transport of the MBP reporter. Fig. 2 E shows that variants that start at residues 130 or 158 of Sco2149 can clearly direct transport of MBP in a Tat-dependent manner because they allow the cells to ferment maltose only in the presence of an active Tat system. If residue 154 was used as the starting position, weak transport activity was also seen, and a variant protein starting at residue 148 was not active. Western blotting of these constructs shows that the poorer Tat signal peptides were generally associated with lower expression or stability of the fusion protein (Fig. S2). However, collectively these results indicate that the Tat machinery can recognize and integrate TM3 of Sco2149 into the membrane.

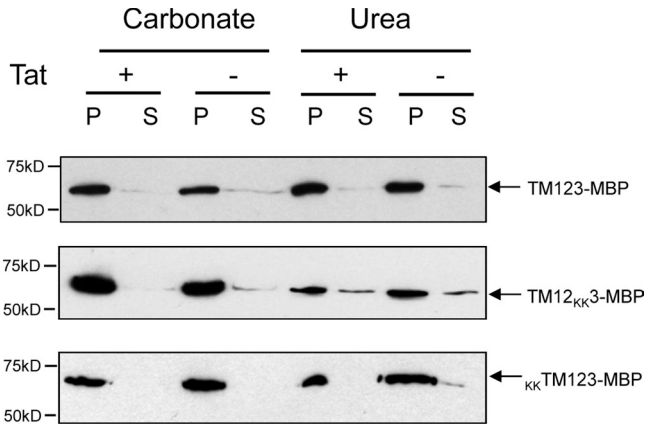

Figure 3. **The TM123-MBP fusion protein is integrated into the membrane in the absence of the Tat machinery.** Crude membranes were prepared from *E. coli* strains HS3018-A and HS3018-A *ΔtatABC* producing TM123-MBP, TM12$_{KK}$3-MBP, or $_{KK}$TM123-MBP as described in Materials and methods. The crude membranes were incubated with either 0.2 M Na_2CO_3 or 4 M urea followed by recovery of the membrane pellet by ultracentrifugation. The presence of the fusion protein in the wash supernatant (S) and pelleted membrane (P) was analyzed by immunoblotting using anti-MBP antiserum.

The first two transmembrane domains of Sco2149 integrate into the membrane in the absence of the Tat machinery

As demonstrated in Fig. 2, the Tat machinery appears to interact with the third transmembrane domain of Sco2149 to transport the globular domain to the periplasmic side of the membrane. Furthermore, evidence was presented which might suggest that the first two transmembrane domains of the protein are still inserted in the membrane in the absence of the Tat machinery. To investigate this further, we isolated crude membrane fractions from an *E. coli* *tat*$^+$ or a *tat*$^-$ strain producing the TM123-MBP fusion protein. The crude membranes were then washed with 0.2 M carbonate or 4 M urea to investigate whether the protein could be extracted from the membrane with either of these treatments. As shown in Fig. 3 (top), the full-length construct was clearly observed in the pelleted membrane fraction after either of these washes, with almost no protein being detected in the wash supernatant. Importantly, the same result was observed irrespective of whether the cells had a functional Tat system. In agreement with this, we also saw exclusive localization of the TM123-AmiA fusion protein in the membrane fraction, and again this protein was resistant to carbonate extraction (Fig. S3).

Identical observations were made when the $_{KK}$TM123-MBP fusion protein (which carries a twin lysine pair replacing the lysine-arginine motif before TM1) was analyzed (Fig. 3, bottom). The behavior of the TM12$_{KK}$3-MBP fusion protein (which has a twin lysine substitution of the twin arginine motif preceding TM3) was also broadly similar to that of the unmutated fusion protein, except that a small fraction of the protein was extractable from the membrane with urea (but not with carbonate; Fig. 3, middle). The reasons for this slight difference in behavior are not entirely clear. Nonetheless, these results clearly show that there is stable integration of the TM123-MBP (and TM123-AmiA) fusion protein into the membrane in the absence of the Tat machinery. Collectively with our previous observations,

Published October 8, 2012

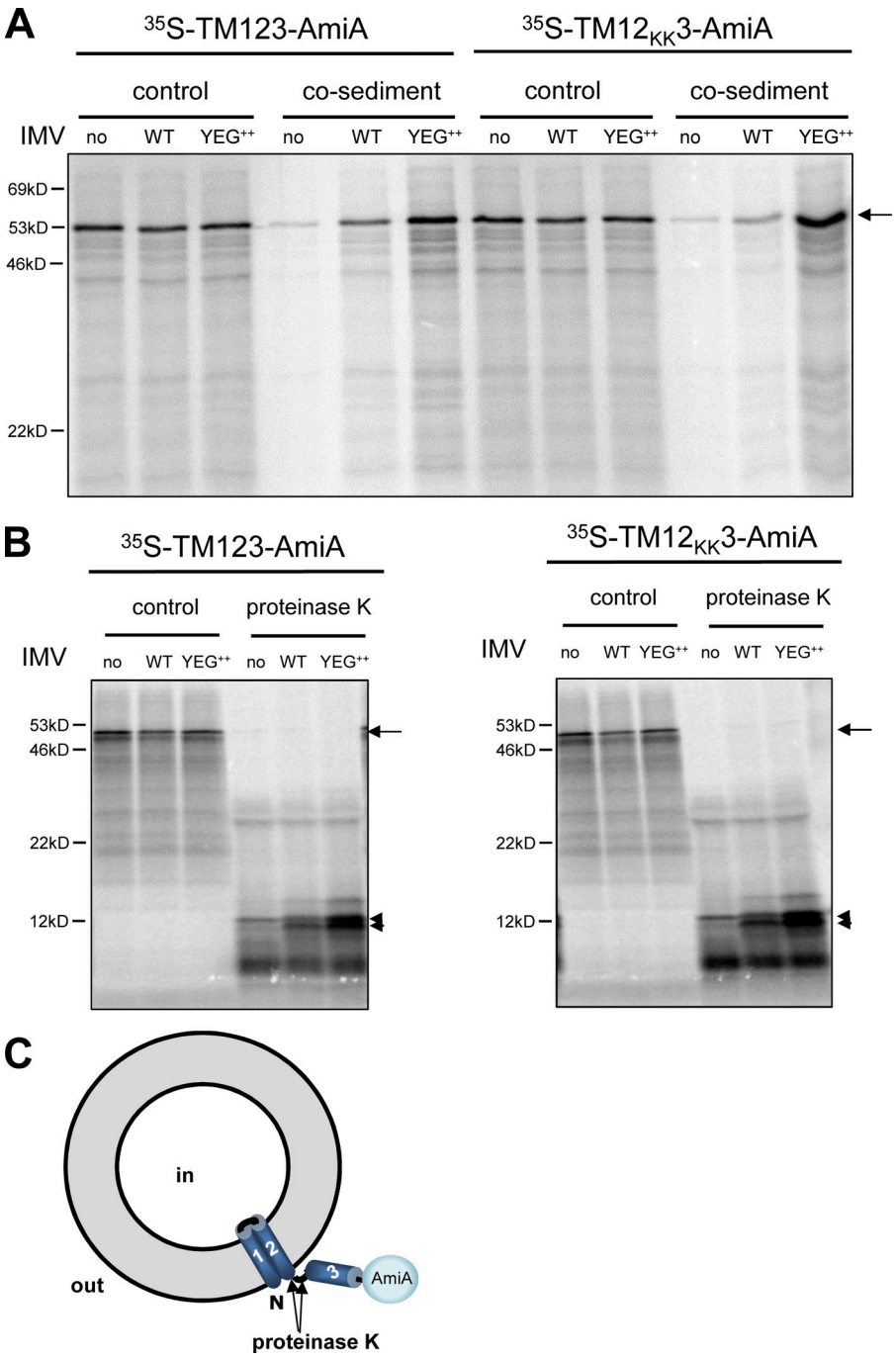

Figure 4. **The Sec pathway facilitates integration of the TM123-AmiA fusion protein into inverted membrane vesicles.** (A) The TM123-AmiA fusion co-sediments with IMVs containing elevated levels of SecYEG. Constructs TM123-AmiA and $TM12_{KK}3$-AmiA were synthesized in vitro in the presence of [^{35}S]methionine and either buffer alone (no), or IMVs (to a final concentration of 0.2 mg/ml protein) derived from strain SF100 harboring plasmid pET302 (WT) or pET2302 that overproduces SecYEG (YEG^{++}). The synthesis reaction was performed for 20 min at 37°C. 10% of the reaction mixture was removed to confirm that protein synthesis was similar between the different samples (lanes labeled "control"). The remaining reaction mixture was treated with 6 M urea (to remove peripherally bound protein), and the vesicles were sedimented by high-speed centrifugation. The pelleted vesicles were resuspended in Laemmli buffer (lanes labeled cosediment), and samples were analyzed by SDS-PAGE and autoradiography. (B) Proteinase K digestion of IMVs containing TM123-AmiA. Samples were prepared as described in A except that instead of sedimenting the samples they were treated with proteinase K. The arrow indicates the full-length protein and the arrowheads indicate protease-resistant fragments. (C) Predicted topology of TM123-AmiA in IMVs. The arrows indicate likely proteinase K–sensitive sites in the linker region between TMs 2 and 3.

these findings clearly indicate that the first two transmembrane domains of Sco2149 are integrated into the membrane by cellular machinery other than the Tat system, and that the Tat system is required to integrate TM3 into the membrane and for the translocation of the C-terminal globular domain.

The Sec pathway and YidC participate in the insertion of the first two transmembrane domains of the Rieske protein

To examine whether the Sec pathway played any role in the assembly of Sco2149 in *E. coli*, we characterized the targeting and insertion of an in vitro synthesized Sco2149 fusion protein into inverted inner membrane vesicles (IMVs). For these experiments, we chose not to use the TM123-MBP fusion protein because MBP itself is normally a Sec substrate and interacts with the Sec chaperone SecB (Gannon et al., 1989). Instead we used the TM123-AmiA fusion protein because AmiA is a natural Tat substrate and should not be expected to interact with Sec pathway components.

The TM123-AmiA construct and the variant carrying the twin lysine substitution of the twin arginine motif adjacent to TM3 were synthesized in vitro in the presence of ^{35}S-labeled methionine. Also present in the synthesis reaction were IMVs containing either wild type or greatly overproduced levels of SecYEG (Fig. S4 A) to allow for the insertion of the labeled protein into the membrane. The amount of inserted TM123-AmiA

Published October 8, 2012

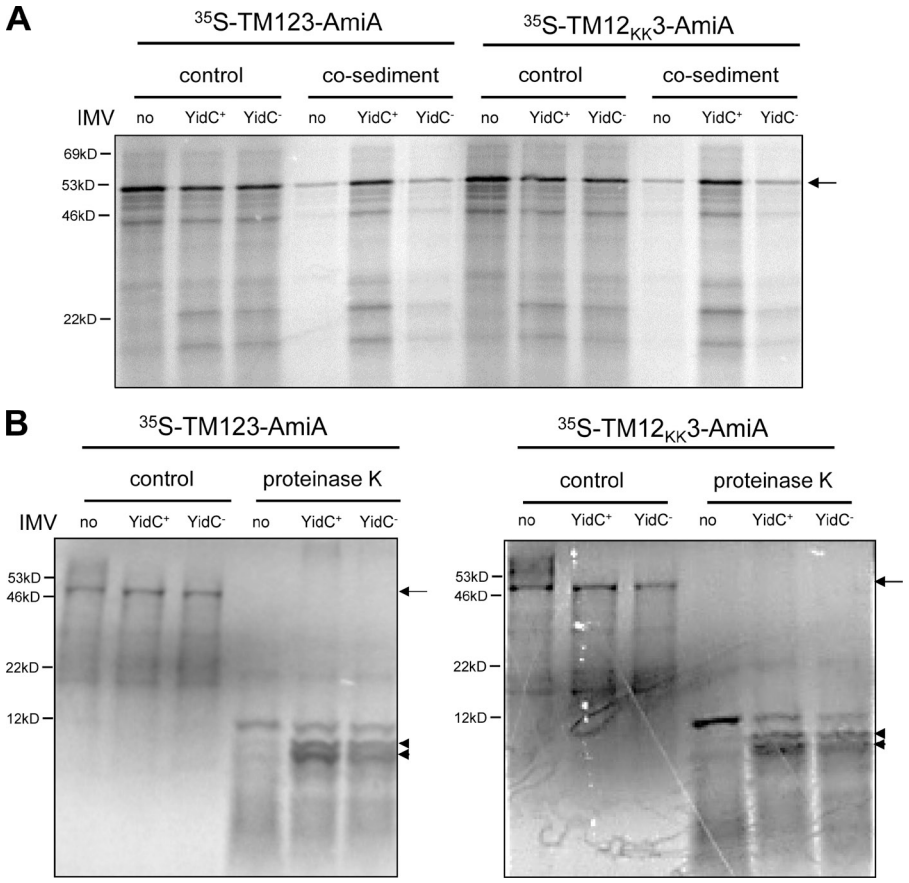

Figure 5. **YidC also facilitates integration of the TM123-AmiA fusion protein into inverted membrane vesicles.** (A) The TM123-AmiA fusion cosediments with IMVs containing elevated levels of YidC. Constructs TM123-AmiA and $TM12_{KK}3$-AmiA were synthesized in vitro in the presence of [^{35}S]methionine and either buffer alone (no) or IMVs (to a final concentration of 0.4 mg/ml protein) derived from strain FTL10 grown under conditions where the chromosomal copy of *yidC* was depleted ($YidC^-$) or the same conditions but where YidC was co-overproduced from a plasmid ($YidC^+$). The synthesis reaction was performed for 20 min at 37°C. 10% of the reaction mixture was removed to confirm that protein synthesis was similar between the different samples (lanes labeled "control"). The remaining reaction mixture was treated with 6 M urea (to remove peripherally bound protein), and the vesicles were sedimented by high-speed centrifugation. The pelleted vesicles were resuspended in Laemmli buffer (lanes labeled cosediment), and the samples were analyzed by SDS-PAGE and autoradiography. (B) Proteinase K digestion of IMVs containing TM123-AmiA. Samples were prepared as described in A, except that instead of sedimenting the samples they were treated with proteinase K. The reaction was stopped by addition of Laemmli buffer and samples were analyzed by SDS-PAGE and autoradiography. The arrows indicate the full-length protein and the arrowheads indicate protease-resistant fragments.

was subsequently assessed by sedimentation of the vesicles after treatment with urea to remove nonintegral proteins. A control insertion experiment using the previously characterized SecYEG substrate ^{35}S-labeled FtsQ (van der Laan et al., 2004b) confirmed that increased insertion of FtsQ was observed in vesicles containing overproduced SecYEG (Fig. S4 B).

As shown in Fig. 4 A, clearly detectable TM123-AmiA fusion protein was cosedimented with the IMVs prepared from the SecYEG wild-type strain, and substantially more of the fusion protein was present when the vesicles contained elevated levels of the Sec proteins. It is likely that this protein is integrated into the membrane via the first two transmembrane domains, as in vitro translocation by the Tat pathway is not observed in vesicles containing normal cellular levels of Tat components (Yahr and Wickner, 2001; Alami et al., 2002). Indeed a variant of TM123-AmiA containing a twin lysine substitution of the twin arginine motif ($TM12_{KK}3$-AmiA) showed essentially the same behavior; i.e., it was also strongly cosedimented with the Sec-overproducing IMVs (Fig. 4 A).

To address the topology of the fusion protein, the in vitro transcription/translation/insertion reaction was treated with proteinase K and analyzed by SDS-PAGE. After protease treatment, resistant bands running just below 12 kD were observed, which increased in intensity upon SecYEG overexpression (Fig. 4 B). The sizes of these bands correspond closely to the predicted size of the first two transmembrane domains, which strongly suggests that these were integrated into the membrane while TM3 was not and that the AmiA domain was degraded by the protease (Fig. 4 C). Collectively, these results clearly demonstrate that the Sec pathway participates in the integration of the first two transmembrane domains of Sco2149 into the membrane.

To analyze whether YidC was also required for the membrane assembly of Sco2149, we examined the insertion of the TM123-AmiA fusion protein into YidC-depleted IMVs prepared from the *E. coli* strain FTL10 (Hatzixanthis et al., 2003). Control insertion experiments, which were performed using the YidC substrate ^{35}S-labeled Foc (van der Laan et al., 2004a), confirmed increased insertion of Foc in the presence of YidC, as expected (Fig. S4 C). It is apparent that when YidC is depleted, much less of the TM123-AmiA fusion protein associates with the vesicles (Fig. 5 A), and, additionally, less membrane integrated fusion protein is observed upon treatment with proteinase K, as is evident from the reduced levels of the characteristic bands below 12 kD (Fig. 5 B). Collectively, these results clearly demonstrate that the SecYEG translocon and YidC participate in the integration of the first two transmembrane domains of the *S. coelicolor* Rieske protein into the membrane. It is also possible that there might be promiscuous targeting of the fusion protein to either SecYEG or YidC, which has been reported recently for some *E. coli* multispanning membrane proteins (Welte et al., 2012).

No crosstalk between the Sec and Tat systems during integration of the Rieske protein

To investigate whether there are any specific features of TM1 and/or TM2 of the Rieske protein that influence the Tat-dependent

Published October 8, 2012

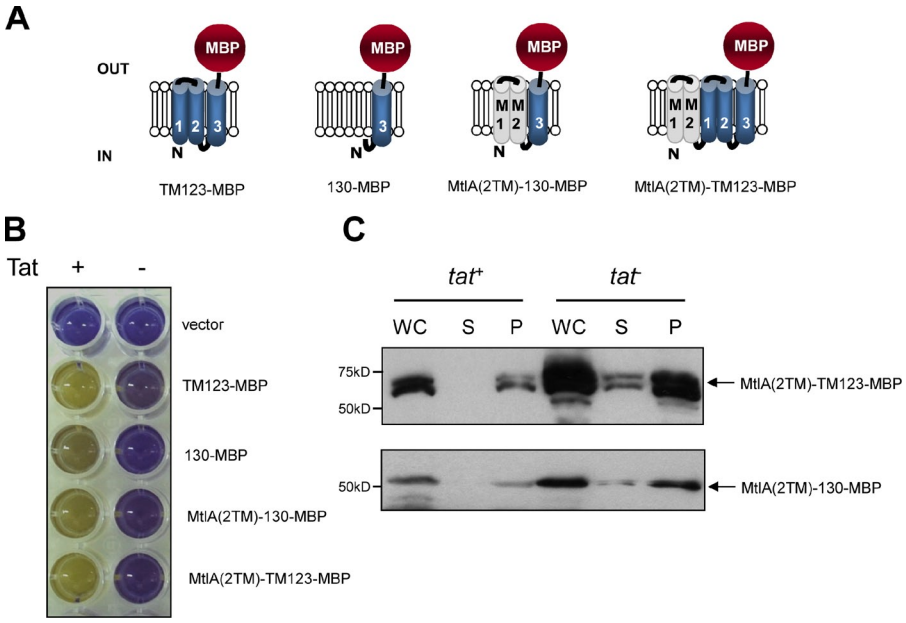

Figure 6. **No crosstalk between the Sec and Tat translocases during Rieske assembly.** (A) Cartoon representation of the chimeric constructs used in these experiments. (B) *E. coli* strain HS3018-A (deleted for *malE*) and an otherwise isogenic *tatABC* mutant strain containing pBAD24 (vector) or pBAD24, producing the Sco2149-MBP fusion protein (TM123-MBP), the first two TMs of MtlA fused to the Sco2149-MBP fusion protein (MtlA(2TM)-TM123-MBP), and MBP fused to TM3 of Sco2149 (130-MBP) or the first two TMs of MtlA fused to the Sco2149 TM3-MBP construct (MtlA(2TM)-130-MBP). These were cultured on maltose indicator broth containing bromocresol purple. (C) Crude membranes were prepared from *E. coli* strains HS3018-A and HS3018-A *ΔtatABC* producing MtlA(2TM)-TM123-MBP or MtlA(2TM)-130-MBP followed by recovery of the membrane pellet by ultracentrifugation. The presence of the fusion protein in whole cells (WC), the wash supernatant (S), and pelleted membrane (P) was analyzed by immunoblotting using anti-MBP antiserum.

assembly of TM3, these transmembrane domains were genetically replaced by the first two transmembrane segments of an unrelated membrane protein, MtlA, to give the construct MtlA(2TM)-130-MBP (Fig. 6 A). As shown in Fig. 6 B, the presence of the MtlA transmembrane domains did not alter the targeting behavior of the reporter protein: the periplasmic localization of the MBP domain remained strictly Tat dependent, and the fusion protein was stable and present in the membrane when the Tat machinery was lacking (Fig. 6 C). It can therefore be concluded that there is no cryptic information in TM1 or TM2 of Sco2149 that influences interaction of TM3 with the Tat pathway, and that the Sec-dependent helices are integrated independently of the Tat-dependent helix with no crosstalk between the two systems.

We next investigated the effect of increasing the overall hydrophobicity of the construct by increasing the number of transmembrane domains before the Tat-dependent TM. The first two TMs of MtlA were fused to the entire TM123-MBP construct to give MltA(2TM)-TM123-MBP (Fig. 6 A), which has five transmembrane domains. As shown in Fig. 6 B, the translocation of MBP still remained strictly Tat dependent. The complete fusion protein was relatively stable (although some breakdown of this construct to give a protein of slightly smaller mass was apparent) and was again integrated into the membrane when the Tat machinery was absent (Fig. 6 C). We therefore conclude that increasing the overall hydrophobicity of the protein does not influence the dual targeting and that translocation of the MBP domain remains strictly Tat dependent, whereas the insertion of all but the final transmembrane domain depends on Sec/YidC, but not on the Tat pathway.

Discussion

In this study, we have shown that the Sec and Tat translocons are able to function together to assemble a polytopic membrane protein, and a model summarizing these data are presented in Fig. 7. Our results clearly show that the first two transmembrane domains of the Sco2149 protein, when produced in *E. coli*, are recognized and integrated into the membrane by the Sec pathway, with the assistance of the YidC insertase. Although we do not know with absolute certainty that the Rieske protein follows the same pathway for its assembly in *Streptomyces*, we feel that it is highly likely, as ongoing work has shown that the native protein is integrated into the membrane in a *S. coelicolor tat* mutant strain (unpublished data). This argues that a second translocon, most likely Sec, also participates in membrane integration in the native organism. Moreover, although an equivalent dual-targeted substrate native to *E. coli* has so far not been recognized, there is clearly no impediment to the Sec and Tat pathways from this organism co-operating to assemble a single membrane protein.

It is highly likely that targeting to the Sec machinery is cotranslational, through interaction of the first (and most hydrophobic) transmembrane segment with SRP. This is supported by the observation that we can replace the first two transmembrane domains of Sco2149 with those of a bona fide SRP substrate, MtlA, and maintain the functional assembly of a Sco2149-MBP reporter protein. Moreover, we could also increase the overall hydrophobicity of the protein by fusing two additional transmembrane domains, and the correct topology of the fusion protein would still be maintained. It is not clear if and for how long polytopic membrane proteins remain Sec translocon-associated after their first hairpin has integrated into the membrane, but the results presented here clearly provide an example of an integration intermediate that very likely has to leave the Sec translocon before it can interact with the Tat machinery.

It is interesting to note that despite having similar hydrophobicity to the third transmembrane segment of MtlA, the Sec machinery clearly does not suffice to correctly position TM3 of Sco2149. If the insertion of the first two TMs is, as we suspect, cotranslational, then there must be features within the protein sequence that prevent the cotranslational insertion of TM3 and

Published October 8, 2012

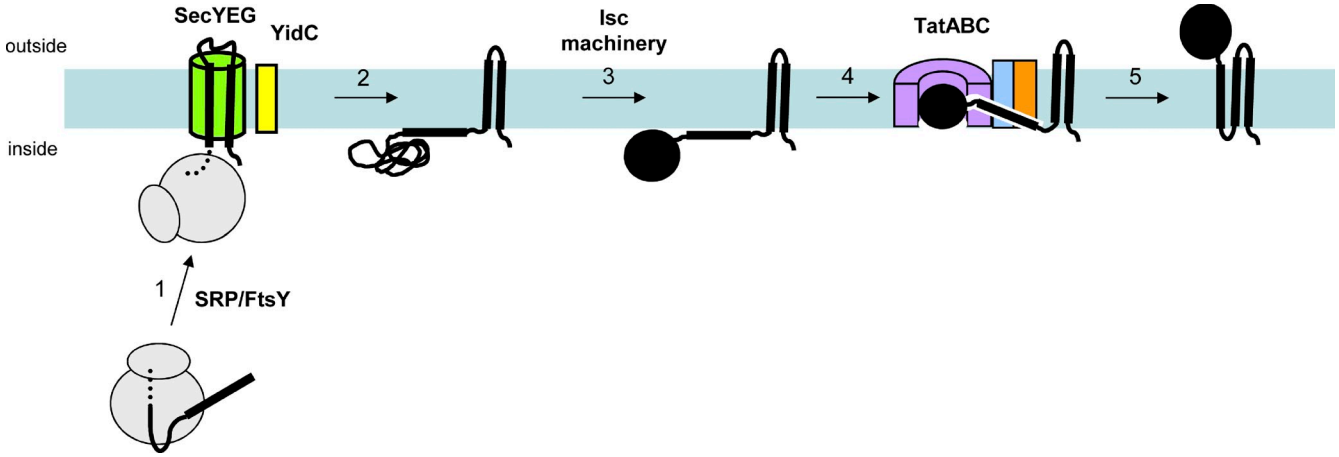

Figure 7. **Model for the biogenesis of the *S. coelicolor* Rieske protein.** (1) SRP binds to the first hydrophobic segment of Sco2149 emerging from the ribosome, and guides the complex to the Sec machinery. (2) The first two TMs of Sco2149 are inserted into the membrane cotranslationally. (3) The iron-sulfur cluster is inserted into Sco2149, leading to folding of the globular domain. (4) The Tat system translocates the Fe-S domain. (5) Fully assembled Sco2149 is released into the membrane, where it can interact with its partner subunits to form the cytochrome bc_1 complex.

drive release of the ribosome from the Sec translocon. This is essential, as the native globular domain of Sco2149 binds a 2Fe-2S cluster that is necessary for its electron transfer function. Therefore, translocation of TM3 and the iron-sulfur cluster domain is strictly posttranslational, and as expected from prior knowledge of bacterial and plant Rieske protein, assembly is dependent on the Tat pathway. When the Tat machinery is absent, or if the conserved arginines of the Tat recognition motif are substituted to lysines, the first two TMs of Sco2149 are inserted into the membrane, but TM3 is not and the globular reporter domain is not transported across the membrane. These findings indicate that when the native route of transport is blocked, TM3 cannot be correctly integrated into the membrane by any of the other protein insertion machineries, including YidC.

Clearly there are features within Sco2149 that prevent a functional interaction of TM3 with the Sec machinery, and presumably that also facilitate the recognition of the internal twin arginine signal sequence by the Tat system. To our knowledge, this is the first example of a natural Tat substrate protein that is tethered to the membrane and that does not have a free N terminus. This would point to the cytoplasmic loop region between TM2 and TM3 as being critical, perhaps as a signal for the Sec machinery, but also to permit recognition of the twin arginine signal sequence by the Tat pathway. Inspection of this loop sequence from several actinobacterial Rieske proteins (Fig. S5) shows that there is surprisingly little absolute sequence conservation. However the linker length is very similar (43 amino acids between the predicted end of TM2 and the twin arginine motif for all of the examples in Fig. S5), and it is striking to note that there is a highly conserved RH motif (where the arginine is invariant and the histidine very highly conserved) at a defined position 28 amino acids away from the first arginine of the twin arginine motif. Moreover the stretch of amino acids between the conserved RH and RR sequences appears to be structurally conserved as an α-helix. Finally, the loop regions all appear to contain at least four negatively charged amino acids between the end of TM2 and the RH motif, with an invariant glutamate situated 10 amino acids C-terminal to the end of TM2. It will be interesting in the future to examine which of these features, if any, function as a stop transfer sequence and which might facilitate recognition of the tethered substrate by Tat system.

Materials and methods

Strain and plasmid construction and growth conditions

The strains and plasmids used in this study are listed in Tables 1 and 2. *E. coli* strains HS3018-AΔ*tatABC* and MCDSSACΔ*tatABC* were derived via P1 transduction of the apramycin-marked Δ*tatABC* allele from strain BW25113 Δ*tatABC*::Apra (Lee et al., 2006) into HS3018-A or MCDSSAC, respectively. *E. coli* strains were grown aerobically at 37°C in Luria Bertani (LB) medium unless stated otherwise. Where required, antibiotics were used at final concentrations of 50 µg/ml apramycin, 100 µg/ml ampicillin, 25 µg/ml chloramphenicol, and 50 µg/ml kanamycin. For growth on SDS, *E. coli* cultures were normalized to an OD_{600} of 0.5, and 10 µl was spotted onto LB medium containing 1% SDS and grown overnight at 37°C. For growth on maltose-bromocresol purple broth, LB medium was supplemented with 0.002% bromocresol purple (Roth), 0.4% maltose, 0.1% L-arabinose, and 10 mM $CaCl_2$. Growth was performed in 96-well plates where each well (containing 200 µl of maltose-bromocresol purple broth) was inoculated with 5 µl of preculture and incubated for 24 h at 37°C without agitation. Photographs of 96-well plates and colonies on agar were captured as JPG files using a digital camera (DX AF-S NIKKOR 18-55 mm; Nikon). JPG files were imported into Photoshop (Adobe) for cropping but otherwise were not processed.

Oligonucleotides used for PCR amplification or site-directed mutagenesis are listed in Table S1. Site-directed mutations were generated using the Quick-Change method (Agilent Technologies) according to the manufacturer's instructions. All clones generated were confirmed by DNA sequencing.

All plasmids used and constructed in this study are listed in Table 2. To produce a fusion of the three TM segments of Sco2149 with MBP, DNA encoding the first 185 amino acids of Sco2159 was PCR amplified using oligonucleotides Rieskestart and Rieskemid and M145 chromosomal DNA as a template, then digested with NcoI and XbaI. This was ligated into similarly digested pBAD24 (an ampicillin-resistant plasmid with an M13 replicon giving tightly controlled expression of cloned genes regulated by arabinose) to give pTM123. DNA encoding the mature region of MBP (aa 27–396) was amplified by PCR using oligonucleotides MBPFor and MBPrev and MC4100 chromosomal DNA as a template. The purified fragment was digested with XbaI and HindIII and subsequently cloned into similarly digested pTM123 to give pTM123-MBP. The amino acid substitutions R54K or RR161-162KK in Sco2149 were generated using the primer pairs 5RieskeKRKK/3RieskeKRKK or 5RieskeRRKK/5RieskeRRKK, respectively, to give plasmids p_{KK}TM123-MBP and pTM12$_{KK}$3-MBP.

Published October 8, 2012

Table 1. **Strains used and constructed in this study**

Strain	Genotype	Source
DH5α	φ80d*lac*ZΔM15, *recA1*, *endA1*, *gyrA96*, *thi*-1, *hsdR17*(rK-, mK+) *supE44*, *relA1*, *deoR*, Δ(*lacZYA-argF*) U169	Laboratory stock
JM109	F′ *traD36 proA*$^+$*B*$^+$ *lacI*^{q} Δ*(lacZ)M15/ Δ(lac-proAB) glnV44 e14*$^-$ *gyrA96 recA1 relA1 endA1 thi hsdR17*	Laboratory stock
HS3018	F-Δ*lacU169 araD139 rpsL150 relA1 ptsF rbs flbB5301 malT* (Con)-*1* Δ*malE444*	Shuman, 1982
HS3018-A	As HS3018, ara$^+$	Caldelari et al., 2008
HS3018-AΔ*tatABC*	As HS3018-A but Δ*tatABC*::Apra	This study
MC4100	F-Δ*lacU169 araD139 rpsL150 relA1 ptsF rbs flbB5301*	Casadaban and Cohen, 1979
MCDSSAC	As MC4100, *amiA*Δ2-33 *amiC*Δ2-32	Ize et al., 2003
MCDSSACΔ*tatABC*	As MCDSSAC, Δ*tatABC*::Apra	This study
FTL10	As MC4100, ara$^+$, Δ*yidC, attB*::(*araC*$^+$, P_{BAD}, *yidC*$^+$) Kan^R)	Hatzixanthis et al., 2003
SF100	F- Δ*lacX74 galE galK thi rpsL* (*strA*) Δ*phoA* (*PvuII*) Δ(*ompT- entF*)	Baneyx and Georgiou, 1990

To produce a fusion of the three TM segments of Sco2149 with AmiA, DNA encoding the mature region of AmiA (aa 33–289), was amplified by PCR using the oligonucleotides 5XbaIAmiAmat and 3HindIIIAmiAmat, and MC4100 chromosomal DNA as a template. The purified PCR fragment was digested with XbaI and HindIII and subsequently cloned into similarly digested pTM123 or pTM12KK3 to give plasmids pTM123-AmiA and pTM12KK3-AmiA, respectively. The construct pTM123-(AxA)AmiA contains DNA coding for aa 32–289 of AmiA fused to MBP, which was amplified by PCR using oligonucleotides 5xbaIAxAAmiA and 3HindIIIAmiAmat, digested XbaI and HindIII, and cloned into similarly digested pTM123. The DNA encoding the Sco2149-AmiA fusions from these three constructs was subsequently moved into vector pSU18 (a pACYC184 derivative specifying chloramphenicol resistance and carrying P_{lac}) to be produced under control of the *lac* promoter. This was achieved by excision of DNA encoding the Sco2149-AmiA fusions by digestion with EcoRI and HindIII and ligation into similarly digested pSU18 (Bartolomé et al., 1991) to give plasmids pSU-TM123-AmiA, pSU-$TM12_{KK}$3-AmiA, and psU-TM123-(AxA)AmiA.

For in vitro insertion experiments, the Sco2149-AmiA fusion was produced from plasmid pET22b+, an expression vector with T7 promoter specifying ampicillin resistance. To achieve this, DNA fragments covering Sco2149 (aa 1–185) and Sco2149 (aa 1–185; RR161-162KK) were amplified using oligonucleotides 5EcoRNdeRieske and Rieskemid and

Table 2. **Plasmids used and constructed in this study**

Plasmid	Relevant features	Source
pBAD24	Cloning vector for expression of genes under control of the *araBAD* promoter	Guzman et al., 1995
pTM123-MBP	pBAD24 producing aa 1–185 of Sco2149 fused to aa 27–396 of *E. coli* MBP	This study
$pTM12_{KK}$3-MBP	pTM123-MBP with substitution of aa 161–162 of Sco2149 from RR to KK	This study
p_{KK}123-MBP	pTM123-MBP with substitution of aa 54 of Sco2149 from R to K	This study
p130-MBP	pBAD24, producing aa 130–185 of Sco2149 fused to aa 27–396 of *E. coli* MBP	This study
p148-MBP	pBAD24, producing aa 148–185 of Sco2149 fused to aa 27–396 of *E. coli* MBP	This study
p154-MBP	pBAD24, producing aa 154–185 of Sco2149 fused to aa 27–396 of *E. coli* MBP	This study
p158-MBP	pBAD24, producing aa 158–185 of Sco2149 fused to aa 27–396 of *E. coli* MBP	This study
$p158_{KK}$-MBP	pBAD24, 158-MBP with exchange of aa 161–162 RR into KK	This study
pMltA(2TM)-130-MBP	pBAD24 producing a fusion protein comprising aa 1–86 of *E. coli* MltA, aa 130–185 of Sco2149 and aa 27–396 of *E. coli* MBP	This study
pMltA(2TM)-TM123-MBP	pBAD24 producing a fusion protein comprising aa 1–86 of *E. coli* MltA, aa 1–185 of Sco2149 and aa 27–396 of *E. coli* MBP	This study
pSU18	Cm^R	Bartolomé et al., 1991
pSUAmiA	pSU18, *amiA*$^+$	Ize et al., 2003
pTM123-AmiA	pBAD24 producing aa 1–185 of Sco2149 fused to aa 33–289 of *E. coli* AmiA	This study
pSU-TM123-AmiA	pSU18 producing aa 1–185 of Sco2149 fused to aa 33–289 of *E. coli* AmiA	This study
$pTM12_{KK}$3-AmiA	pTM123-AmiA with substitution of aa 161–162 of Sco2149 from RR to KK	This study
pSU-$TM12_{KK}$3-AmiA	pSU-TM123-AmiA with substitution of aa 161–162 of Sco2149 from RR to KK	This study
psU-TM123-(AxA)AmiA	pSU18 producing aa 1–185 of Sco2149 fused to aa 32–289 of *E. coli* AmiA	This study
pET22b+	Amp^{R}T7 promoter preceding multiple cloning site	EMD Millipore
pET-TM123-AmiA	pET22b, producing aa 1–185 of Sco2149 fused to aa 33–289 of *E. coli* AmiA	This study
pET-$TM12_{KK}$3-AmiA	pET-TM123-AmiA with substitution of aa 161–162 of Sco2149 from RR to KK	This study
pET302	pTRC99A-derived vector containing *lacZ*R behind the *trc* promoter, a His tag and an enterokinase site	van der Does et al., 1998
pET2302	pET302 containing *secYEG* behind *trc* promoter with N-terminally His-tagged SecY	de Keyzer et al., 2002
pTRC99A	Amp^R *lac* promoter preceding multiple cloning site	Amann et al., 1988
pTRC99AYidC	pTRC99A carrying *yidC*	Saller et al., 2009
pQE60	Cloning vector for producing histidine tagged proteins	QIAGEN
pQESco2149	pQE60 producing Sco2149 with a C-terminal hexa-histidine tag	This study

Published October 8, 2012

either pTM123 or pTM12KK3-MBP as a template. The forward primer was designed to introduce at the 5′ end an EcoRI followed by an NdeI restriction site, the latter covering the start codon of Sco2149. These fragments were initially recloned into pTM123-AmiA after digestion with EcoRI and XbaI. Finally, DNA covering the entire fusion protein was excised by digestion with NdeI and HindIII and ligated into similarly digested pET22b+ to give plasmids pET-TM123-AmiA and pET-TM12$_{KK}$3-AmiA.

To produce proteins comprising TM3 of Sco2149 fused to MBP, DNA covering aa 130–185, aa 148–185, or aa 154–185 was amplified by PCR using oligonucleotide Rieskemid as a reverse primer and 5EcoRI3rdT130, 5EcoRI3rdT148, or 5EcoRI3rdT154 as a forward primer. The purified PCR-fragments were digested with EcoRI and XbaI and cloned into similarly digested pTM123-MBP to give p130-MBP, p148-MBP, and p154-MBP. For the fusion protein containing aa 158–185 of Sco2149 or its twin lysine variant, the encoding DNA was amplified with Rieskemid as a reverse primer and either 5EcoRI3rdT158 or 5EcoRI3rdT158KK as a forward primer. The purified PCR fragments were digested with NcoI and XbaI and cloned into similarly digested pBAD24. Subsequently, the *malE* fragment was excised from pTM123 by digestion with XbaI and HindIII and ligated into the pBad24-Sco2149 (aa 158–185) vectors to give plasmids p158-MBP and p158$_{KK}$-MBP.

Fusion proteins comprising the first two transmembrane domains of *E. coli* MtlA fused to variants of Sco2149-MBP were constructed as follows. DNA covering aa 1–86 of MtlA was amplified by PCR using oligonucleotides mtA2TMEcoRI and mltA2TMNcoI, and M4100 chromosomal DNA as a template. The purified fragment was digested with EcoRI and NcoI and cloned into either p130-MBP or pTM123, which had been similarly digested. The resulting intermediate plasmids were further digested with EcoRI and XbaI and the released fragments encoding mltA(2TM)-130 or mltA2TM-TM123 were ligated into pTM123-MBP that had been similarly digested. The resulting clones were designated pMltA(2TM)-130-MBP and pMltA(2TM)-TM123-MBP.

For overproduction of Sco2149, the encoding gene was cloned into pQE60, an expression vector with T5 promoter specifying ampicillin resistance. This was achieved after amplification of *sco2149* using oligonucleotides RiskQEwtFor and RiskQErev and M145 chromosomal DNA as a template. The resulting fragment was digested with NcoI and BamHI and ligated into similarly digested pQE60 to give plasmid pQESco2149.

Subcellular fractionation

Sphaeroplasts were generated using the lysozyme/EDTA method of Hatzixanthis et al. (2003), using *E. coli* cells that had been induced for plasmid-encoded gene expression at an OD_{600} of 0.3–0.5 by addition of L-arabinose (0.02% final concentration) for 3 h before harvesting. Equivalent numbers of cells from each sample were used (as judged by measuring the optical density at 600 nm) for spheroplast formation. In brief, cell pellets were resuspended in 20% (wt/vol) sucrose and 50 mM Tris-HCl, pH 7.6. EDTA was added to 5 mM (final concentration) together with lysozyme (0.6 mg/ml final concentration), and the mixture was incubated at room temperature for 30 min. To test protein accessibility, spheroplasts were treated with proteinase K to a final concentration of 0.5 mg/ml for 40 min at room temperature. The reaction was stopped by the addition of 0.5 mM phenylmethylsulfonyl fluoride followed by sample precipitation with 15% TCA. Pellets were solubilized in equivalent volumes of 0.1 N NaOH, mixed with SDS loading buffer (Bio-Rad Laboratories), and analyzed via SDS-PAGE (Laemmli, 1970) and Western blotting (Towbin et al., 1979).

Membrane and soluble cell fractions were prepared in buffer A (50 mM Tris/HCl, pH 7.6, 10% glycerol, and protease inhibitor cocktail; Bio-Rad Laboratories) using *E. coli* cells that were grown overnight at 30°C in LB supplemented with 0.2% L-arabinose. Cells were lysed by sonication and the crude cell extract recovered followed centrifugation at 14,000 *g* for 10 min. The extract was treated with either 0.2 M Na_2CO_3 or 4 M urea (final concentrations) for 20 min followed by ultracentrifugation for 1 h at 200,000 *g*. The soluble fraction, containing a mixture of cytoplasm and periplasm was removed and retained. The pellet fraction (containing inner and outer membranes) was resuspended in buffer A.

In vitro protein insertion experiments

IMVs were prepared and membrane protein insertion experiments were performed essentially as described by de Keyzer et al. (2007). In vitro synthesis and insertion reactions were performed for 20 min at 37°C using T7 polymerase (Fermentas) and Easytag express protein labeling mix (PerkinElmer) in the presence of 0.2 mg/ml IMVs prepared from *E. coli* strain SF100 harboring the plasmids pET302 (van der Does et al., 1998) or pET2302 (de Keyzer et al., 2002), or 0.4 mg/ml IMVs, prepared from *E. coli* strain FTL10 (Hatzixanthis et al., 2003) transformed with pTRC99A or pTRC99AYidC to obtain YidC-depleted or nondepleted cells (Saller et al., 2009). A small sample of the reaction mixture was removed at this stage as a synthesis control. After synthesis, the whole mixture was treated with 6 M urea (final concentration) and incubated for a further 30 min on ice. Sedimentation of the vesicles was performed by ultracentrifugation at 100,000 *g* for 30 min, after which the supernatant was removed and the pellet was resuspended in Laemmli buffer. Alternatively, the reactions were treated with 0.4 mg/ml proteinase K for 30 min on ice, after which they were TCA-precipitated and resuspended in Laemmli buffer. Samples were analyzed by SDS-PAGE and autoradiography.

Immunological analysis

For Western blot analysis, protein samples were separated by SDS-PAGE, electroblotted, and probed with primary antibodies raised against the *E. coli* proteins MBP fusion (purchased from New England Biolabs, Inc.), TatA (a polyclonal anti–rabbit anti-serum raised against the purified *E. coli* TatA protein; Sargent et al., 2001), or LepB (generous gift of J.-W. de Gier, Stockholm University, Stockholm, Sweden), or against Sco2149 (see the following paragraph). Immunodetection was performed by using the Chemiluminescent substrate (EMD Millipore; Merck) with a peroxidase-conjugated anti–mouse or anti–rabbit IgG (Bio-Rad Laboratories). Band intensities were quantified using QuantityOne software (Bio-Rad Laboratories).

Purification of Sco2149-His$_6$

A C-terminally his-tagged variant of Sco2149 was purified from *E. coli* inclusion bodies as follows: *E. coli* strain JM109 harboring pQESco2149 along with pRKISC (which encodes the *E. coli* iron-sulfur cluster insertion machinery; Nakamura et al., 1999) was grown aerobically at 37°C in 3 liters of LB medium. Production of Sco2149-His$_6$ was induced once the culture had reached an OD_{600} of 0.3, by addition of 1 mM IPTG. Induction was allowed to proceed for 3 h, after which the cells were harvested and the cell pellet was resuspended in 20 ml buffer A. Cells were lysed by sonication, the lysate was centrifuged at 17,400 *g* for 10 min, and the pellet (2.5 mg) was resuspended in 25 ml buffer F (20 mM Tris/HCl, pH 7.5, 0.15 M NaCl, 25 mM Imidazole, 2 mM DTT, and 0.05% dodecylmaltoside [DDM]) supplemented with a protease inhibitor cocktail (Roche) and containing 5 M urea. The sample was incubated for 45 min at room temperature, after which it was loaded onto a 5 ml His-TrapHP column (GE Healthcare) that had been pre-equilibrated with Ni^{2+} as described by the manufacturer. Unbound protein was washed through the column with buffer F containing 5 M urea. To allow renaturation of bound protein, the urea concentration in wash buffer F was slowly reduced to zero. Bound proteins were subsequently eluted by application of a 0.025–0.5 M gradient of imidazole in buffer F. The eluted protein fraction was analyzed by SDS-PAGE, and fractions containing Sco2149-His$_6$ (which were brown in color) were pooled and supplied to Dundee Cell Products to raise antisera in rabbits.

Online supplemental material

Fig. S1 shows proteinase K accessibility of the control proteins LepB (periplasmic-facing control) and TatA (cytoplasmic-facing control) in sphaeroplasts containing TM123-MBP. Fig. S2 shows the expression levels of different constructs containing TM3 of Sco2149 fused to MBP. Fig. S3 demonstrates that The TM123-AmiA fusion protein is integrated into the membrane in a carbonate-resistant manner in the absence of the Tat machinery. Fig. S4 shows analysis of IMVs containing overproduced SecYEG for SecY, SecE/G, and YidC levels, and proteinase K digestion of IMVs containing in vitro synthesized control proteins FtsQ or Foc. Fig. S5 shows an amino acid sequence alignment of the loop region between TMD2 and TMD3 from different actinobacterial Rieske proteins. Table S1 shows oligonucleotides used in this study. Online supplemental material is available at http://www.jcb.org/cgi/content/full/jcb.201204149/DC1.

We thank Holger Kneuper for constructing the *E. coli* strain MCDSSACΔ*tatABC* and Greetje Berrelkamp-Lahpor for the isolation of YidC-depleted IMVs. We acknowledge Philip Lee, Peter Daldrop, and Fiona Lim for their assistance with making some of the plasmids used in this work, Dr. Jan-Willem de Gier for providing us with anti-LepB antiserum, and Ben Berks, Frank Sargent, and David Widdick for helpful discussions.

This work is funded by a Deutsche Forschungsgemeinschaft postdoctoral fellowship FL 712/1-1 to R. Keller, Medical Research Council grant G0901653, and Chemical Sciences, which is subsidized by the Netherlands Foundation for Scientific Research.

Submitted: 27 April 2012
Accepted: 10 September 2012

Published October 8, 2012

References

Alami, M., D. Trescher, L.F. Wu, and M. Müller. 2002. Separate analysis of twin-arginine translocation (Tat)-specific membrane binding and translocation in *Escherichia coli*. *J. Biol. Chem.* 277:20499–20503. http://dx.doi.org/10.1074/jbc.M201711200

Amann, E., B. Ochs, and K.J. Abel. 1988. Tightly regulated *tac* promoter vectors useful for the expression of unfused and fused proteins in *Escherichia coli*. *Gene*. 69:301–315. http://dx.doi.org/10.1016/0378-1119(88)90440-4

Bachmann, J., B. Bauer, K. Zwicker, B. Ludwig, and O. Anderka. 2006. The Rieske protein from *Paracoccus denitrificans* is inserted into the cytoplasmic membrane by the twin-arginine translocase. *FEBS J.* 273:4817–4830. http://dx.doi.org/10.1111/j.1742-4658.2006.05480.x

Baneyx, F., and G. Georgiou. 1990. In vivo degradation of secreted fusion proteins by the *Escherichia coli* outer membrane protease OmpT. *J. Bacteriol.* 172:491–494.

Bartolomé, B., Y. Jubete, E. Martínez, and F. de la Cruz. 1991. Construction and properties of a family of pACYC184-derived cloning vectors compatible with pBR322 and its derivatives. *Gene*. 102:75–78. http://dx.doi.org/10.1016/0378-1119(91)90541-I

Berks, B.C. 1996. A common export pathway for proteins binding complex redox cofactors? *Mol. Microbiol.* 22:393–404. http://dx.doi.org/10.1046/j.1365-2958.1996.00114.x

Blaudeck, N., P. Kreutzenbeck, R. Freudl, and G.A. Sprenger. 2003. Genetic analysis of pathway specificity during posttranslational protein translocation across the *Escherichia coli* plasma membrane. *J. Bacteriol.* 185:2811–2819. http://dx.doi.org/10.1128/JB.185.9.2811-2819.2003

Caldelari, I., T. Palmer, and F. Sargent. 2008. *Escherichia coli tat* mutant strains are able to transport maltose in the absence of an active *malE* gene. *Arch. Microbiol.* 189:597–604. http://dx.doi.org/10.1007/s00203-008-0356-8

Casadaban, M.J., and S.N. Cohen. 1979. Lactose genes fused to exogenous promoters in one step using a Mu-*lac* bacteriophage: *in vivo* probe for transcriptional control sequences. *Proc. Natl. Acad. Sci. USA*. 76:4530–4533. http://dx.doi.org/10.1073/pnas.76.9.4530

Cline, K., and S.M. Theg. 2007. The Sec and Tat protein translocation pathways in chloroplasts. *In* Molecular Machines Involved in Protein Transport Across Cellular Membranes. Vol. XXV. R.E. Dalbey, Koehler, C.M., and Tamanoi, F., editors. Elsevier, London. 463–492.

De Buck, E., L. Vranckx, E. Meyen, L. Maes, L. Vandersmissen, J. Anné, and E. Lammertyn. 2007. The twin-arginine translocation pathway is necessary for correct membrane insertion of the Rieske Fe/S protein in *Legionella pneumophila*. *FEBS Lett.* 581:259–264. http://dx.doi.org/10.1016/j.febslet.2006.12.022

de Keyzer, J., C. van der Does, J. Swaving, and A.J.M. Driessen. 2002. The F286Y mutation of PrlA4 tempers the signal sequence suppressor phenotype by reducing the SecA binding affinity. *FEBS Lett.* 510:17–21. http://dx.doi.org/10.1016/S0014-5793(01)03213-6

de Keyzer, J., M. van der Laan, and A.J.M. Driessen. 2007. Membrane protein insertion and secretion in bacteria. *Methods Mol. Biol.* 390:17–31. http://dx.doi.org/10.1007/978-1-59745-466-7_2

Driessen, A.J.M., and N. Nouwen. 2008. Protein translocation across the bacterial cytoplasmic membrane. *Annu. Rev. Biochem.* 77:643–667. http://dx.doi.org/10.1146/annurev.biochem.77.061606.160747

du Plessis, D.J., N. Nouwen, and A.J.M. Driessen. 2006. Subunit *a* of cytochrome *o* oxidase requires both YidC and SecYEG for membrane insertion. *J. Biol. Chem.* 281:12248–12252. http://dx.doi.org/10.1074/jbc.M600048200

Gannon, P.M., P. Li, and C.A. Kumamoto. 1989. The mature portion of *Escherichia coli* maltose-binding protein (MBP) determines the dependence of MBP on SecB for export. *J. Bacteriol.* 171:813–818.

Guzman, L.M., D. Belin, M.J. Carson, and J. Beckwith. 1995. Tight regulation, modulation, and high-level expression by vectors containing the arabinose P_{BAD} promoter. *J. Bacteriol.* 177:4121–4130.

Hatzixanthis, K., T. Palmer, and F. Sargent. 2003. A subset of bacterial inner membrane proteins integrated by the twin-arginine translocase. *Mol. Microbiol.* 49:1377–1390. http://dx.doi.org/10.1046/j.1365-2958.2003.03642.x

Ize, B., N.R. Stanley, G. Buchanan, and T. Palmer. 2003. Role of the *Escherichia coli* Tat pathway in outer membrane integrity. *Mol. Microbiol.* 48:1183–1193. http://dx.doi.org/10.1046/j.1365-2958.2003.03504.x

Laemmli, U.K. 1970. Cleavage of structural proteins during the assembly of the head of bacteriophage T4. *Nature*. 227:680–685. http://dx.doi.org/10.1038/227680a0

Lee, P.A., G.L. Orriss, G. Buchanan, N.P. Greene, P.J. Bond, C. Punginelli, R.L. Jack, M.S. Sansom, B.C. Berks, and T. Palmer. 2006. Cysteine-scanning mutagenesis and disulfide mapping studies of the conserved domain of the twin-arginine translocase TatB component. *J. Biol. Chem.* 281:34072–34085. http://dx.doi.org/10.1074/jbc.M607295200

Molik, S., I. Karnauchov, C. Weidlich, R.G. Herrmann, and R.B. Klösgen. 2001. The Rieske Fe/S protein of the cytochrome b_6/f complex in chloroplasts: missing link in the evolution of protein transport pathways in chloroplasts? *J. Biol. Chem.* 276:42761–42766. http://dx.doi.org/10.1074/jbc.M106690200

Nagamori, S., I.N. Smirnova, and H.R. Kaback. 2004. Role of YidC in folding of polytopic membrane proteins. *J. Cell Biol.* 165:53–62. http://dx.doi.org/10.1083/jcb.200402067

Nakamura, M., K. Saeki, and Y. Takahashi. 1999. Hyperproduction of recombinant ferredoxins in *escherichia coli* by coexpression of the *ORF1-ORF2-iscS-iscU-iscA-hscB-hs cA-fdx-ORF3* gene cluster. *J. Biochem.* 126:10–18. http://dx.doi.org/10.1093/oxfordjournals.jbchem.a022409

Niebisch, A., and M. Bott. 2001. Molecular analysis of the cytochrome bc_1-aa_3 branch of the *Corynebacterium glutamicum* respiratory chain containing an unusual diheme cytochrome c1. *Arch. Microbiol.* 175:282–294. http://dx.doi.org/10.1007/s002030100262

Niebisch, A., and M. Bott. 2003. Purification of a cytochrome bc-aa3 supercomplex with quinol oxidase activity from *Corynebacterium glutamicum*. Identification of a fourth subunity of cytochrome aa3 oxidase and mutational analysis of diheme cytochrome c1. *J. Biol. Chem.* 278:4339–4346. http://dx.doi.org/10.1074/jbc.M210499200

Palmer, T., and B.C. Berks. 2012. The twin-arginine translocation (Tat) protein export pathway. *Nat. Rev. Microbiol.* 10:483–496.

Saller, M.J., F. Fusetti, and A.J.M. Driessen. 2009. *Bacillus subtilis* SpoIIIJ and YqjG function in membrane protein biogenesis. *J. Bacteriol.* 191:6749–6757. http://dx.doi.org/10.1128/JB.00853-09

Sargent, F. 2007. Constructing the wonders of the bacterial world: biosynthesis of complex enzymes. *Microbiology*. 153:633–651. http://dx.doi.org/10.1099/mic.0.2006/004762-0

Sargent, F., U. Gohlke, E. De Leeuw, N.R. Stanley, T. Palmer, H.R. Saibil, and B.C. Berks. 2001. Purified components of the *Escherichia coli* Tat protein transport system form a double-layered ring structure. *Eur. J. Biochem.* 268:3361–3367. http://dx.doi.org/10.1046/j.1432-1327.2001.02263.x

Scotti, P.A., M.L. Urbanus, J. Brunner, J.W. de Gier, G. von Heijne, C. van der Does, A.J.M. Driessen, B. Oudega, and J. Luirink. 2000. YidC, the *Escherichia coli* homologue of mitochondrial Oxa1p, is a component of the Sec translocase. *EMBO J.* 19:542–549. http://dx.doi.org/10.1093/emboj/19.4.542

Serek, J., G. Bauer-Manz, G. Struhalla, L. van den Berg, D. Kiefer, R. Dalbey, and A. Kuhn. 2004. *Escherichia coli* YidC is a membrane insertase for Sec-independent proteins. *EMBO J.* 23:294–301. http://dx.doi.org/10.1038/sj.emboj.7600063

Shuman, H.A. 1982. Active transport of maltose in *Escherichia coli* K12. Role of the periplasmic maltose-binding protein and evidence for a substrate recognition site in the cytoplasmic membrane. *J. Biol. Chem.* 257:5455–5461.

Stanley, N.R., T. Palmer, and B.C. Berks. 2000. The twin arginine consensus motif of Tat signal peptides is involved in Sec-independent protein targeting in *Escherichia coli*. *J. Biol. Chem.* 275:11591–11596. http://dx.doi.org/10.1074/jbc.275.16.11591

Summer, E.J., H. Mori, A.M. Settles, and K. Cline. 2000. The thylakoid delta pH-dependent pathway machinery facilitates RR-independent N-tail protein integration. *J. Biol. Chem.* 275:23483–23490. http://dx.doi.org/10.1074/jbc.M004137200

Towbin, H., T. Staehelin, and J. Gordon. 1979. Electrophoretic transfer of proteins from polyacrylamide gels to nitrocellulose sheets: procedure and some applications. *Proc. Natl. Acad. Sci. USA*. 76:4350–4354. http://dx.doi.org/10.1073/pnas.76.9.4350

Van den Berg, B., W.M. Clemons Jr., I. Collinson, Y. Modis, E. Hartmann, S.C. Harrison, and T.A. Rapoport. 2004. X-ray structure of a protein-conducting channel. *Nature*. 427:36–44. http://dx.doi.org/10.1038/nature02218

van der Does, C., E.H. Manting, A. Kaufmann, M. Lutz, and A.J.M. Driessen. 1998. Interaction between SecA and SecYEG in micellar solution and formation of the membrane-inserted state. *Biochemistry*. 37:201–210. http://dx.doi.org/10.1021/bi972105t

van der Laan, M., P. Bechtluft, S. Kol, N. Nouwen, and A.J.M. Driessen. 2004a. F1F0 ATP synthase subunit c is a substrate of the novel YidC pathway for membrane protein biogenesis. *J. Cell Biol.* 165:213–222. http://dx.doi.org/10.1083/jcb.200402100

van der Laan, M., N. Nouwen, and A.J. Driessen. 2004b. SecYEG proteoliposomes catalyze the Deltaphi-dependent membrane insertion of FtsQ. *J. Biol. Chem.* 279:1659–1664. http://dx.doi.org/10.1074/jbc.M306527200

Wagener, N., M. Ackermann, S. Funes, and W. Neupert. 2011. A pathway of protein translocation in mitochondria mediated by the AAA-ATPase Bcs1. *Mol. Cell*. 44:191–202. http://dx.doi.org/10.1016/j.molcel.2011.07.036

Published October 8, 2012

Weiss, J.B., C.H. MacGregor, D.N. Collier, J.D. Fikes, P.H. Ray, and P.J. Bassford Jr. 1989. Factors influencing the in vitro translocation of the *Escherichia coli* maltose-binding protein. *J. Biol. Chem.* 264:3021–3027.

Welte, T., R. Kudva, P. Kuhn, L. Sturm, D. Braig, M. Müller, B. Warscheid, F. Drepper, and H.G. Koch. 2012. Promiscuous targeting of polytopic membrane proteins to SecYEG or YidC by the *Escherichia coli* signal recognition particle. *Mol. Biol. Cell*. 23:464–479. http://dx.doi.org/10.1091/mbc.E11-07-0590

Widdick, D.A., K. Dilks, G. Chandra, A. Bottrill, M. Naldrett, M. Pohlschröder, and T. Palmer. 2006. The twin-arginine translocation pathway is a major route of protein export in *Streptomyces coelicolor*. *Proc. Natl. Acad. Sci. USA*. 103:17927–17932. http://dx.doi.org/10.1073/pnas.0607025103

Yahr, T.L., and W.T. Wickner. 2001. Functional reconstitution of bacterial Tat translocation in vitro. *EMBO J.* 20:2472–2479. http://dx.doi.org/10.1093/emboj/20.10.2472

Published October 8, 2012

Keller et al., http://www.jcb.org/cgi/content/full/jcb.201204149/DC1

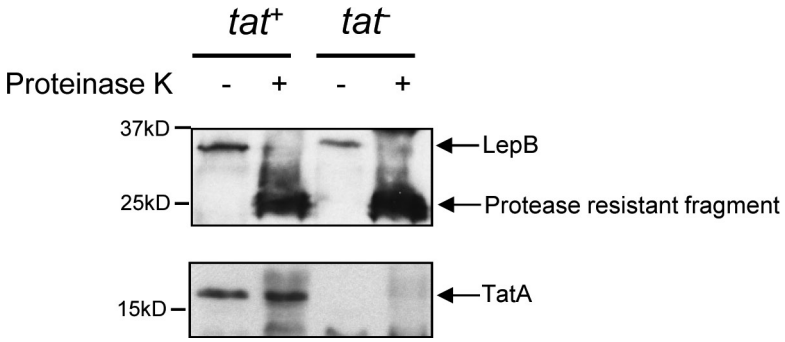

Figure S1. **Proteinase K accessibility of the control proteins LepB and TatA in spheroplasts containing TM123-MBP.** Sphaeroplasts were prepared from HS3018-A or HS3018-AΔ*tatABC* strains producing TM123-MBP. Samples were treated with proteinase K, precipitated with TCA, and analyzed via immunoblotting using anti-LepB or anti-TatA antisera as indicated. Note that LepB is a membrane protein with a large periplasmic globular domain, whereas TatA is a monotopic membrane protein that is only protease accessible from the cytoplasmic side of the membrane. Also note that TatA is not detectable in the *tat*⁻ lanes because the encoding gene is deleted.

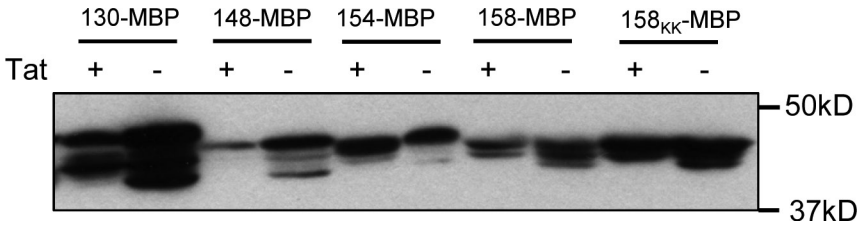

Figure S2. **Expression level of MBP constructs fused to TM3 of Sco2149.** *E. coli* strains HS3018-A and an isogenic *tatABC* mutant producing 130-MBP, 148-MBP, 154-MBP, 158-MBP, or 158_{KK}-MBP were cultured in LB medium containing 0.2% L-arabinose. Cell cultures were normalized using the optical density at 600 nm, and equivalent aliquots were loaded on SDS-PAGE and electroblotted, then fusion proteins were immunodetected using anti-MBP antiserum.

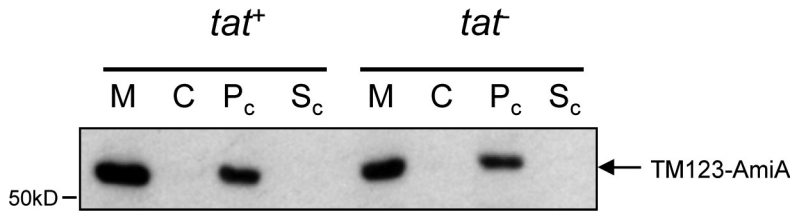

Figure S3. **The TM123-AmiA fusion protein is integrated into the membrane in the absence of the Tat machinery.** Crude membranes (M) and soluble cell extract (C) were prepared from *E. coli* strains MCDSSAC and MCDSSAC Δ*tatABC* producing TM123-AmiA. The crude membranes were incubated with 0.2 M Na_2CO_3 followed by recovery of the membrane pellet (P) and wash supernatant (S) by ultracentrifugation. The presence of the fusion protein in each of the fractions was analyzed by immunoblotting using anti-Sco2149 antiserum.

Published October 8, 2012

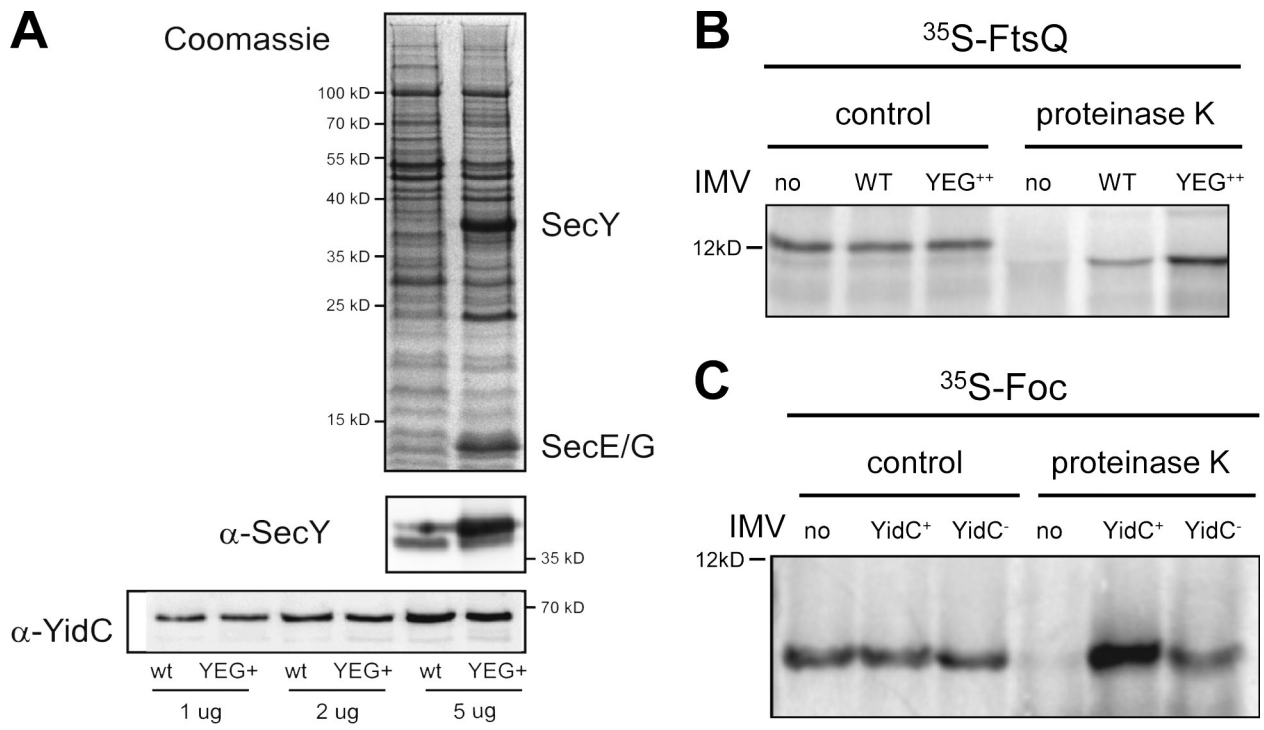

Figure S4. **Analysis of IMVs containing overproduced SecYEG.** (A, top) SDS-PAGE analysis of IMVs from *E. coli* strain SFT100 carrying the empty vector pET302 (left) or pET2302 (which overproduces SecYEG; right). 10 µg of protein was loaded in each lane. Overproduced bands corresponding to SecY and SecE/G are indicated. (A, middle) 2 µg of the same samples were separated by SDS-PAGE and probed with an anti-SecY antibody. (A, bottom) Different amounts of the vesicles obtained from the wild-type and SecYEG-overproducing strains were probed with an anti-YidC antibody. The results show that the levels of YidC are not increased in the vesicles containing overproduced SecYEG. (B) Proteinase K digestion of IMVs containing in vitro synthesized FtsQ. FtsQ was synthesized in vitro in the presence of [^{35}S]methionine and either buffer alone (no), IMVs (to a final concentration of 0.2 mg/ml protein) derived from strain SF100 carrying the empty plasmid vector pET302 (WT), or SF100 harboring plasmid pET2302 that overproduces SecYEG (YEG^{++}). The synthesis reaction was performed for 20 min at 37°C. 10% of the reaction mixture was removed to confirm that protein synthesis was similar between the different samples (lanes labeled "control"). The remaining reaction mixture was treated with proteinase K (0.4 mg/ml) for 30 min on ice. The reaction was stopped by the addition of Laemmli buffer and samples were analyzed by SDS-PAGE and autoradiography. (C) Proteinase K digestion of IMVs containing in vitro synthesized Foc. Foc was synthesized in vitro in the presence of [^{35}S]methionine and either buffer alone (no), IMVs (to a final concentration of 0.4 mg/ml protein) derived from strain FTL10 grown under conditions where the chromosomal copy of *yidC* was depleted (YidC^{-}), or under the same conditions but where YidC was coproduced from a plasmid (YidC^{+}). The synthesis reaction was performed for 20 min at 37°C. 10% of the reaction mixture was removed to confirm that protein synthesis was similar between the different samples (lanes labeled "control"). The remaining reaction mixture was treated with proteinase K (2 mg/ml) for 30 min at room temperature and analyzed by SDS-PAGE and autoradiography.

Published October 8, 2012

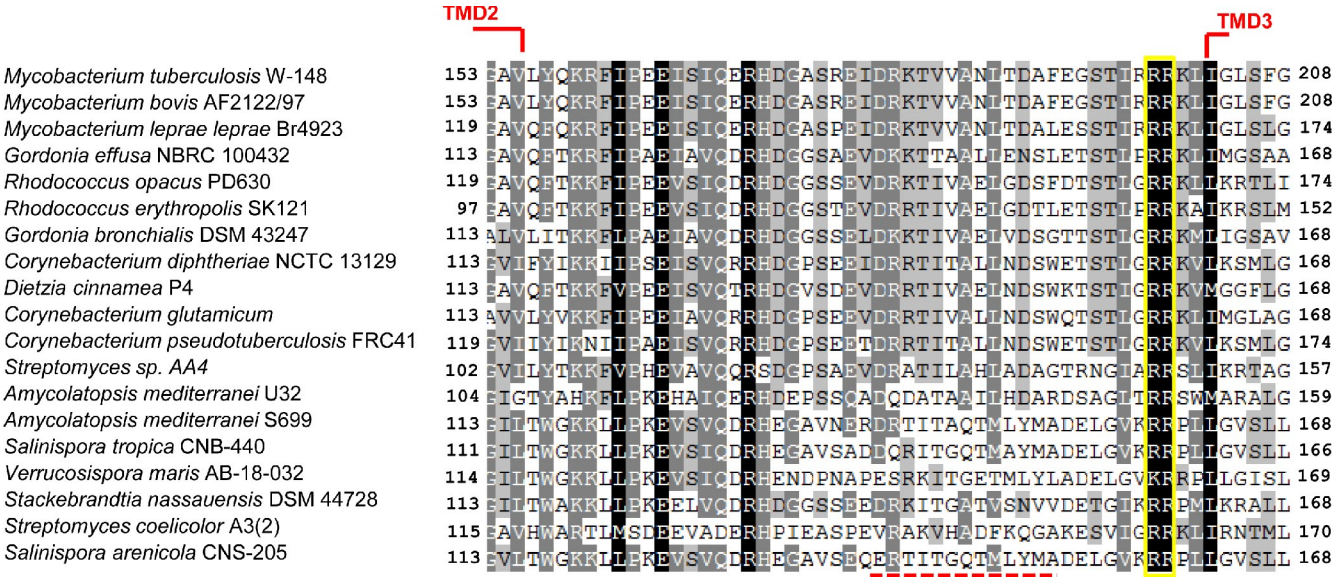

Figure S5. **Amino acid sequence alignment of the loop region between TMD2 and TMD3 from different actinobacterial Rieske proteins.** Sequences were aligned using ClustalW. The likely end position of TMD2 and the start of TMD3 are indicated above the alignment, and the twin arginine motif is highlighted with a yellow box. The dotted red line below the alignment marks the position of predicted α-helical secondary structure determined using Jpred3. The differences in shading (from gray to black) refer to the level of amino acid conservation between the different species (with black indicating absolute conversion).

Table S1. **Oligonucleotides used in this study**

Name	Sequence (5′–3′)
RiskQEwtFor	CGCCC**ATG**GCGAGTAGCCAAGACATTCCAGAAG
RiskQErev	GCGCGGATCCTCCGCGCTCCCAGTAAGC
Rieskestart	GCGCC**ATG**GCGAGTAGCCAAGACATTCCAGAAG
Rieskemid	GCGCTCTAGAGCGCACCAGGAGGACGCC
MBPfor	GCGCTCTAGAAAAATCGAAGAAGGTAAACTGG
MBPrev	GCGCAAGCTTTTACTTGGTGATACGAGTC
5EcoRI3rdT130	GCGAATTCACC**ATG**GCCGACGAGCGTCACCCGATC
5EcoRI3rdT148	GCGAATTCACC**ATG**GCGGACTTCAAGCAGGGTGCC
5EcoRI3rdT154	GCGAATTCACC**ATG**GCCAAGGAGTCCGTGATCGGG
5EcoRI3rdT158	GCGCC**ATG**GTGATCGGGCGCCGCAAGC
5EcoRI3rdT158KK	GCGCC**ATG**GTGATCGGGAAGAAGAAGCTGATCCGCAACACG
5XbaIAmiAmat	GCGCTCTAGAATCGCCAAAGACGAACTTTTAAAAAC
5xbaIAxAAmiA	GCGCTCTAGAGCCATCGCCAAAGACGAACTTTTAAAAAC
3HindIIIAmiAmat	GCGCAAGCTTTTATCGCTTTTTCGAATGTGCTTTC
5RieskeKRKK	GAGCGGGCCGCCAAGAAGTCCGAGCGCACGGTC
3RieskeKRKK	GACCGTGCGCTCGGACTTCTTGGCGGCCCGCTC
5RieskeRRKK	GCCAAGGAGTCCGTGATCGGGAAGAAGAAGCTGATCCGCAACACG
3RieskeRRKK	CGTGTTGCGGATCAGCTTCTTCTTCCCGATCACGGACTCCTTGGC
5EcoRNdeRieske	GGAGGAATTCCAT**ATG**GCGAGTAGCCAAGACAT
mtlA2TMEcoRI	GGGAATTCACC**ATG**TCATCCGATATTAAGATC
mtlA2TMNcoI	GCCCATGGTGGTGATGGCACCGACTACGCC

Restriction sites are underlined and start codons are shown in bold.